

Structural and Dynamic Alteration of Glycated Human Serum Albumin in Schiff Base and Amadori Adducts: A Molecular Simulation Study

Sittivanichai, Sirin

Faculty of Science, Department of Chemistry, Kasetsart University

Japrungrung, Deanpen

National Nanotechnology Center, National Science and Technology Development Agency

Mori, Toshifumi

Institute for Materials Chemistry and Engineering, Kyushu University

Pongprayoon, Prapasiri

Faculty of Science, Department of Chemistry, Kasetsart University

<https://hdl.handle.net/2324/7159643>

出版情報 : Journal of Physical Chemistry B. 127 (23), pp.5230-5240, 2023-06-02. American Chemical Society

バージョン :

権利関係 : This document is the Accepted Manuscript version of a Published Work that appeared in final form in The Journal of Physical Chemistry B, copyright ©2023 American Chemical Society after peer review and technical editing by the publisher. To access the final edited and published work see Related DOI.



Structural and Dynamic Alteration of Glycated Human Serum Albumin in Schiff Base and Amadori Adducts: A Molecular Simulation Study

Sirin Sittivanichai¹, Deanpen Japrun², Toshifumi Mori^{3,4*}, Prapasiri Pongprayoon^{1,5*}

¹Faculty of Science, Department of Chemistry, Kasetsart University, Chatuchak, Bangkok 10900, Thailand

²National Nanotechnology Center, National Science and Technology Development Agency, Thailand Science Park, Pathum Thani 12120, Thailand

³Institute for Materials Chemistry and Engineering, Kyushu University, Kasuga, Fukuoka 816-8580, Japan

⁴Interdisciplinary Graduate School of Engineering Science, Kyushu University, Kasuga, Fukuoka 816-8580, Japan

⁵Center for Advanced Studies in Nanotechnology for Chemical, Food and Agricultural Industries, KU Institute for Advanced Studies, Kasetsart University, Bangkok 10900, Thailand.

* Corresponding authors:

E-mail: toshi_mori@cm.kyushu-u.ac.jp

Telephone: +81-92-583-7800

E-mail: fsciprpo@ku.ac.th

Telephone: +66-2562-5555

Keywords: Glycated human serum albumin, Human serum albumin, Glycation, Diabetes, MD simulations

Abbreviations:

HSA	Human Serum Albumin
GHSA	Glycated Human Serum Albumin
GLO	Open-chain glucose
GLC	Pyranose glucose
MD	Molecular Dynamics

Abstract

Human Serum Albumin (HSA) is a protein carrier in blood transporting metabolites and drugs. Glycated HSA (GHSA) acts as a potential biomarker for diabetes. Thus, many attempts have been made to detect GHSA. The glycation was reported to damage structure and ligand-binding capability where no molecular detail is available. Recently, the crystal structure of GHSA has been solved where two glucose isomers (pyranose:GLC and open-chain:GLO) are located at Sudlow's site I. GLO was found to covalently bind to K195, while GLC is trapped by non-contact interactions. GHSA exists in two forms (Schiff base (SCH) and Amadori (AMA) adducts), but how both disrupt albumin activity microscopically remains unknown. To this end, molecular dynamics simulations were performed here to explore the nature of SCH and AMA. Both forms are found to alter the main protein dynamics, resulting in (i) the widening of Sudlow's site I entrance, (ii) the size reduction of nine fatty acid-binding pockets, (iii) the enlargement of Sudlow's site I and the shrunken Sudlow's site II, (iv) the enhancement of C34 reactivity, and (v) the change in W214 microenvironment. These unique characteristics found here can be useful for understanding the effect of glycation on albumin function in more detail and designing specific and selective GHSA-detecting strategies.

Introduction

Diabetes mellitus is a disease caused by a group of carbohydrate metabolism disorders which leads to the elevated blood sugar level. People with diabetes have higher risks of serious damages such as heart failure, neuropathy, nephropathy and retinopathy.¹ The efficient determination of the amount of glucose is thus necessary for monitoring and controlling the glucose level. The excess glucose is known to bind to Human Serum Albumin (HSA) via the non-enzymatic glycation during hyperglycemia and form glycated HSA (GHSA).² HSA is the abundant protein carrier found in blood, and is commonly used as an indicator for many diseases including diabetes and renal diseases.^{3,4} GHSA has been suggested to be one of potential diabetes biomarkers⁵ since its level in blood can be used for diabetes screening and monitoring in medical practice.⁶ The GHSA detection can also be employed for patients with kidney and liver problems whose hemoglobin A1c level (which is a common diabetes biomarker) may be inaccurate.

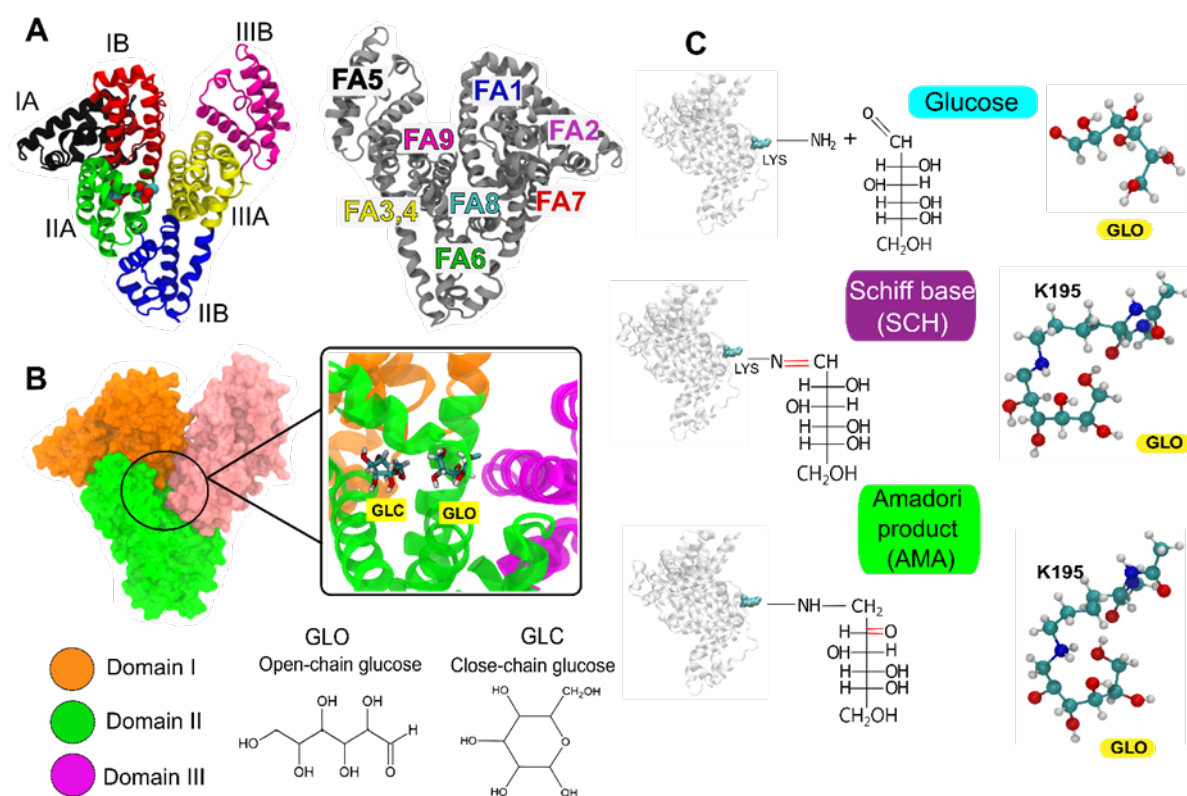


Figure 1 (A) Cartoon view of GHSA with subdomains labels (top). The drug- and fatty acid-binding sites are also labelled. (B) The location of both glucose molecules. Chemical structures of both glucose molecules are also shown at the bottom. (C) Structures of HSA with glucose (top), SCH (middle), and AMA (bottom).

HSA is a roughly spherically heart-shaped protein and consists of 585 amino acids with molecular weight of 66.5 kDa.¹¹ HSA has three domains denoted as domain I, II and III. Each

domain is divided into two subdomains (A and B) which are connected by loop structures (Figure 1A). HSA was suggested to act as the main fatty acid binding protein in blood, although it can also carry various metabolites such as hormones⁸, ions, natural products⁹, and drugs¹⁰⁻¹³. HSA has nine sites for medium-chain fatty acids (C10) (FA1-FA9) and two major drug-binding sites. The latter are denoted as Sudlow's site I (warfarin-azapropazone site) and Sudlow's site II (indole-benzodiazepine site) and are located at subdomains IIA and IIIA¹⁴⁻¹⁶ (Figure 1A), respectively. During diabetes progression, the high level of blood glucose induces the glycation of HSA. Such glycation reaction typically occurs between lysine (sometimes arginines) and glucose, leading to the formation of Schiff base (SCH) and more complex Amadori (AMA) adduct (Figure 1C) before eventually turning into the Advanced Glycation End products (AGEs).^{17, 18} Multiple glycation sites on HSA have been reported. For instance, K12, K64, K195, K199, K205, K233, K281, K439, and K525 have been suggested to be possible glycation sites¹⁹⁻²¹. Recently, the crystal structure of glycated HSA was solved.²² Two glucose molecules (pyranose (cyclic) glucose (GLC) and open-chain glucose (GLO)) were found inside Sudlow's site I where GLO is covalently bound to K195 of HSA via the bond between amine nitrogen on K195 and α -hydroxy carbonyl structure of GLO²² (Figure 1B, C). Yet, the exact form of glycated complex remains unclear. In the early stage of glycation, glucose molecules reversibly transform into SCH and sequentially changes into AMA adduct.^{17, 18} SCH has a half-life of over an hour to days before rearranging into AMA product, which then can exist for weeks to months. Both SCH and AMA forms can thus be found in real samples and act as potential biomarkers.²³ SCH and AMA have been reported to impair structure and ligand-binding affinity²⁴⁻²⁶, while the molecular detail remains obscure. Recently, the antiglycation activity of certain vitamin B was reported²⁷, but how such chemical microscopically interferes the glycation process is unclear. Thus, a molecular insight into the structural impairment of albumin during glycation is crucial, not only to design GHSA detection strategies for effective diabetes monitoring and screening, but also to better understand how glycation alters the ligand-binding affinity of albumin under diabetes conditions.

To date, not only the structural and dynamic properties of the two sugar-bound HSA complexes, i.e. SCH and AMA, remain vague, but the impact of these properties to function remain unclear. To this end, here the structural and dynamic characters of SCH and AMA forms are investigated using molecular dynamics (MD) simulations. This work also reports how glycation alters the microenvironment of drug- and fatty acid-binding sites, which is expected to impact the ligand-binding affinity and structural impairment. The unique

characteristics of both glucose isomers are also revealed. This study thus aims at exploring how the glycation affects structure and ligand-binding capability of albumin.

Materials and Methods

The preparation of glycated human serum albumin (GHSA) topology

The crystal structure of GHSA (PDB:4IW2) containing two glucose molecules (one pyranose (GLC) and one open-chain glucose (GLO)) where GLO is covalently bound to K195 at Sudlow's site I were downloaded from PDB databank.²² The Schiff base (SCH) and Amadori (AMA) configurations were built by modifying GLO-K195 structure using Gaussview -6.1.²⁸ The molecular structures of SCH and AMA forms are displayed in Figure 1C. The electrostatic potential of two GLO-K195 complexes were calculated using density functional theory at B3LYP(6-31G(d)) level using Gaussian16 package²⁹. The electrostatic potentials were used to assign the RESP charges using antechamber from AmberTool20.³⁰ The charges of the two GLO-K195 complexes (SCH and AMA forms) are displayed in Figure S1 of Supplementary Information. The structure of the GLO-lysine complex was further explored to check the dependency of the charges on the structure, where we found only small variation of RESP charges. The crystal structure of GHSA was used as a template for building the GLO-K195 geometry. The AMBER99SB-ILDN³¹, general Amber force field (GAFF)³², and GLYCAM_06 were used for protein, GLO-K195 complex, and non-covalent glucose (GLC), respectively. AMBERTools20³² was used to create the topology files. The conversion tool (ACPYPE) was used to transform AMBER file format to GROMACS topology files.³³

Simulation protocols

MD simulations were carried out using GROMACS2020.7 software package.³⁴ The two GHSA forms were submerged in a 10x10 x10 nm³ cubic box with TIP3P water, and neutralized by counterions. Particle Mesh Ewald (PME) was used for electrostatic treatment³⁵ with a cutoff radius of 1 nm. A 5000-step energy minimization was performed using the steepest descent algorithm. Subsequently, 10-ns equilibrium run was performed under a constant number of particles, pressure, and temperature (NPT) ensemble. The systems were heated to 300 K with a coupling constant of 0.1 ps and the pressure was maintained to 1 bar using the Berendsen thermostat with a coupling constant of 1.0 ps. An isothermal compressibility of 4.5x10⁻⁵ bar⁻¹ in all directions is set. During the equilibrium stage, all heavy atoms were restrained with a constant force of 1000 kJmol⁻¹nm⁻². Long-range electrostatic interactions were calculated, with a fourth-order spline interpolation and a Fourier spacing of 0.16 nm. Each equilibrated structure

was followed by a 500-ns production run, where the restraints on atoms were removed. Each system was repeated twice with different random seeds. In total, four systems were studied (SCH1, SCH2, AMA1, and AMA2). The suffixes of “1” and “2” stand for repeats 1 and 2 in each system. The 2-fs timestep was used for integration. Graphical images were represented by VMD³⁶. Hydrogen bond counts were defined as distance between the donor and acceptor atoms within 0.35 nm and the angle between the donor, hydrogen, and the acceptor atoms below 30°. Protein Allosteric Sites Server (PASSer)³⁷ was used to calculate the cavity sizes in the protein. The secondary structure was analyzed by “do_dssp” option in GROMACS.

Results and Discussions

Collective changes of GHSA upon glycation

First, the structural flexibility and fluctuation are investigated via C_α root-mean-square-deviations (RMSDs) (Figure 2). The structure at 0 ns was used as a reference. Overall, it appears that glycated albumins in both forms induce slightly higher structural flexibility than the native one (RMSD below 0.4 nm in a previous work) (Figure 2A).³⁸ In particular, AMA seems to promote structural flexibility (especially AMA1). This is due to the high flexibility of subdomain IIIB (Figure 2B). This can be confirmed by the smaller C_α RMSD of AMA after by omitting subdomain IIIB (an inset in Figure 2A (right)). Such high flexibility at subdomain IIIB can also be found in ligand-free and sugar-bound HSAs.³⁹ Domain I is also mobile in both SCH and AMA (Figure 2B). Domain I and subdomain IIIB are fluctuating largely in all cases, whereas only subdomain IIB of SCH shows higher flexibility than AMA. In contrast, subdomains IIA and IIIA in both forms are rather rigid. This is due to the presence of bound glucose molecules at Sudlow’s site I (this drug-binding site is located at the interface of subdomains IIA and IIIA).

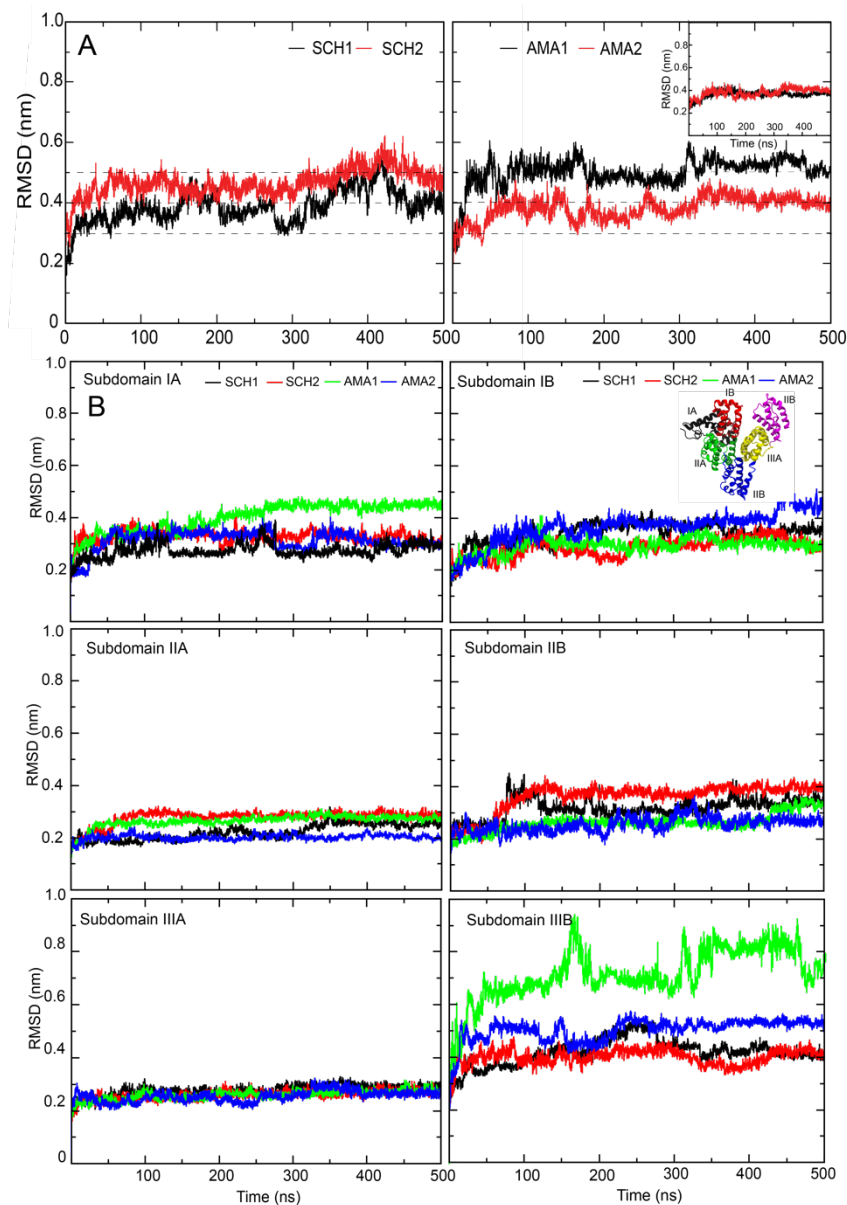


Figure 2 C_{α} RMSDs of the whole protein (A) and each subdomain (B) in all systems. The inset in the upper-right shows the results without subdomain IIIB.

The superimposition of 0 and 500 ns structures (Figures 3A and B) captures the clear inward movement of domain I and subdomain IIIB in all cases. To extract the main protein motion, Principal Component Analysis (PCA) was also performed (Figures 3A, B and S2). Only principal component 1 (PC1) is used from this calculation because it accounts for the main motion (Figure S2 in supplementary information). PC1 clearly reveals the “twisting” motion of domains I and III where the two domains move towards one another (Figure 3AB, and S2 in supplementary information). The presence of covalently bound GLO seems to alter the protein dynamics. Unlike GHSA shown here, domains I and III of native albumins and albumins with non-covalently bound ligands including monosaccharides perform the

scissoring-like movement.³⁹⁻⁴³ This finding confirms that glycation of albumin induces the change in albumin dynamics. Furthermore, the glycation also disrupts the compactness of the protein structure in both SCH and AMA (Figure S3 in supplementary information). Compared to native HSA, the denaturation of protein structure is identified in both cases (Table 1). This structure decomposition is in good agreement with previous experimental studies.^{44, 45} Approximately ~10% helicity is lost in SCH and AMA. These regions seem to mostly decompose into turns (Table 1). The superimpositions of the initial (0 ns) and final (500 ns) structures (Figure 3) clearly show that the helix unfolding occurs at domain I and subdomain IIIB. The glycation clearly triggers the helical decomposition at domains I and III. Such unfolding appears to interfere with the protein dynamics, leading to the “twisting” motion (Figure 3A,B). This also indicates that the twisting motion and helix unfolding are correlated.

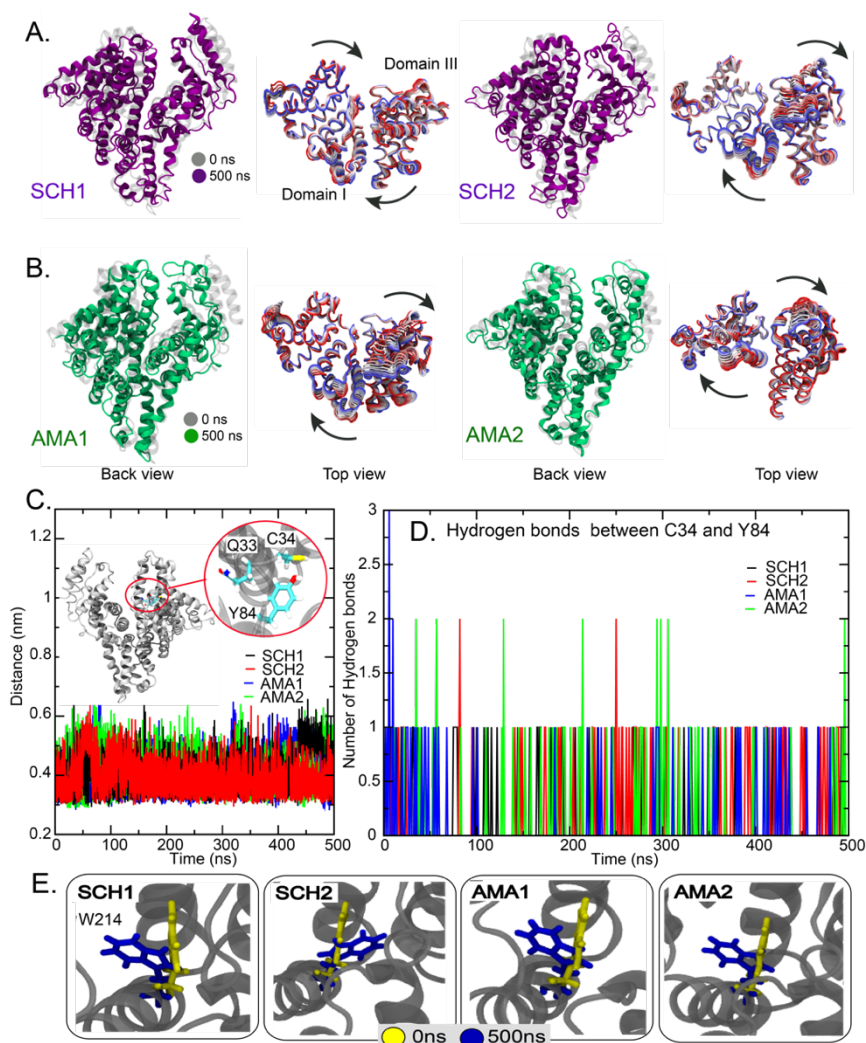


Figure 3 (A, B) Superimposition of GHSA at 0 ns (grey) and 500 ns (magenta for SCH and green for AMA) (left) and the motion of the first principal component (PC1) (right). The motion is displayed in RWB format. (C) Distance between the thiol sulfur atom on C34 and

hydroxyl oxygen on Y84. (D) Number of C34-Y84 hydrogen bonds as a function of time. (E) Reorientation of W214 in the pocket.

Table 1 Percentages of secondary structure of all systems. The data for native HSA was computed from the crystal structure of ligand-free albumin (PDB code: 1AO6). For AMA and SCH, the final snapshot (500ns) of SCH and AMA in each system were used for calculation.

SYSTEM	HELIX (%)	TURN (%)	COIL (%)
NATIVE HSA	68.21	17.44	12.99
SCH1	57.44	26.56	15.88
SCH2	59.91	23.77	15.94
AMA1	58.50	25.99	15.31
AMA2	61.01	24.40	14.42

Furthermore, the reactivity of C34 in each system is explored (Figure 3C,D). In general, albumins contain 17 conserved disulfide bonds to stabilize their structures⁴⁶. Most albumins have one cysteine at position 34 (C34) that is out of the disulfide network. C34 was reported to contribute to the redox homeostasis in the circulation and exert anti-oxidative activity, oxidative stress⁴⁷, and brain rejuvenation. The C34 reactivity varies among albumins depending on the water accessibility to the thiol group. Thus, C34 is of interest for its ability to become an acceptor for a site-selective covalent drug conjugation⁴⁸. In HSA, C34 can interact with its neighbor, Y84, which helps to modulate C34 reactivity and protect C34 from reactions.⁴⁹ On the contrary, Y84 in animal albumins rather interacts with Q33, causing free C34 to be more reactive.^{41, 43, 50} In GHSA, although the short C34-Y84 distances are captured, no permanent C34-Y84 hydrogen bond is found (Figure 3C,D). Only occasional C34-Y84 hydrogen bonds and no Y84-Q33 interaction is observed. Such lack of C34-Y84 interactions in GHSA indicates the more solvent exposed and more reactive environment about C34.

The reorientation of W214, which is a key for measuring spectroscopic characteristics of HSA, is further found (Figure 3E). W214 resides in Sudlow's site I. A presence of bound ligand can alter the dynamic movement of W214, leading to a change in its spectroscopic properties. Thus, the spectroscopic characteristics of W214 is commonly used to determine the ligand-binding capability.^{9, 51-53} Compared to native HSA⁵⁴, the rotameric states of W214 in SCH1, AMA1, and AMA2 differ from that in native HSA (Figure 3E and S4 in supplementary information). This indicates that the change in W214 microenvironment inside Sudlow's site I can make GHSA spectroscopically different from the apo HSA.

Effect of glycation to the ligand-binding sites

Sudlow's sites I and II are known to function as drug carriers. The glycation of HSA was reported to impact both protein structure and function.¹⁹ In our MD trajectories, both glucose isomers were kept inside a pocket in AMA, while the escape of GLC was observed in SCH. To examine the effect of glycation on ligand binding ability, the binding cavities in all GHSA as well as native HSA were computed using PASSer.³⁷ The last snapshots (500 ns) of SCH and AMA were used to predict the binding cavities. The three largest cavities are displayed in red (Sudlow's site I), orange, and yellow VdW surfaces (Figure 4A). Sudlow's site I is found to be the largest binding pocket. This finding agrees well with previous works.^{14,15} Nonetheless, upon glycation, the notable size alteration of ligand-binding pocket is spotted. These changes highlight the impairment of ligand-binding capability of GHSA. The cavity sizes of main drug-binding sites (Sudlow's site I and II) are further investigated by calculating the cavity volumes of Sudlow's site I and II (Figure 4B). As expected, Sudlow's site I remains larger than Sudlow's site II, as is the case in native HSA. However, compared to apo HSA⁴¹, the presence of covalently bound GLO seems to expand the cavity volume at Sudlow's site I, while a slightly smaller size of Sudlow's site II is found in both SCH and AMA. The glycation seems to have more impact on Sudlow's site I than the site II. Further study is required to examine the ligand-binding ability at Sudlow's site II. We note that the escape of GLC in SCH was not caused by the enlargement of the cavity size since both SCH and AMA provide similar size for Sudlow's site I. Further in-depth analyses are discussed in the next section.

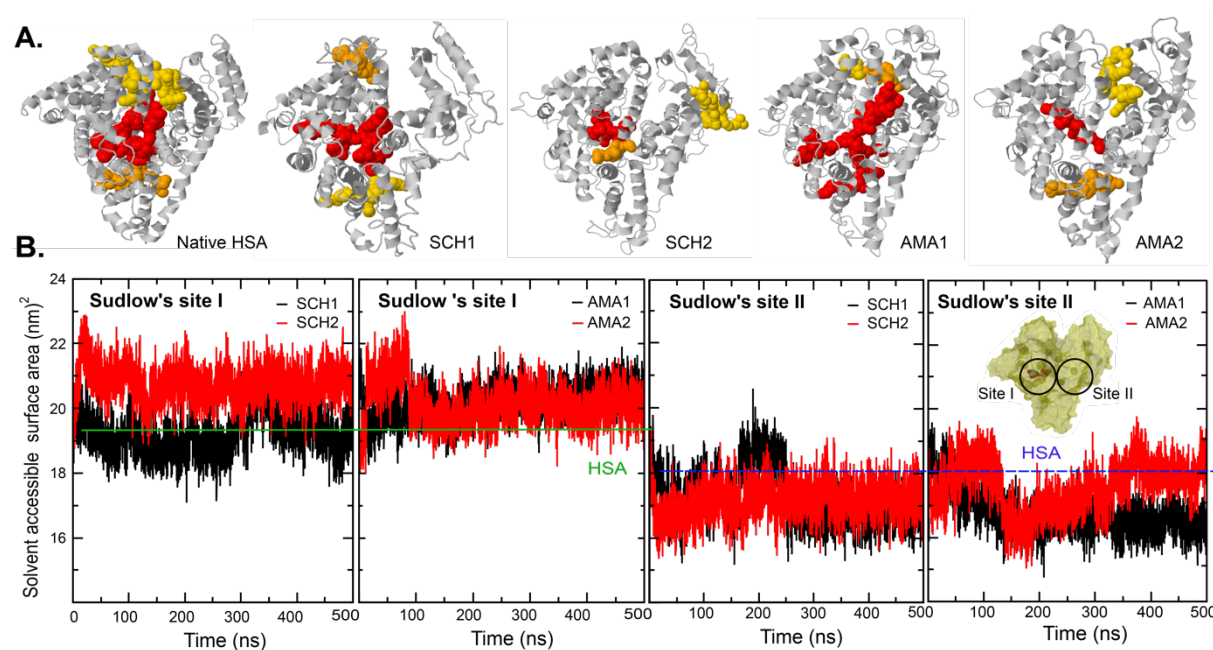


Figure 4 (A) Cartoon views of the native HSA and GHSA at 500 ns with three largest cavities from all systems. The cavities are computed by PASSer.³⁴ The three largest cavities are displayed in red, orange, and yellow VdW surfaces. (B) Solvent accessible surface areas of Sudlow's site I (left two) and II (right two) as a function of time.

Apart from the drug-binding sites, the effect of glycation on fatty acid (FA)-binding sites is also investigated. The solvent accessible surface areas of nine FA-binding sites are computed in comparison to those of native HSA (Table 2). These nine FA-binding sites have been identified for medium chain fatty acids.¹⁶ In Table 2, the severe shrinking of all FA-binding sites is found in all GHSA forms. This suggests the deterioration of FA-binding capability of GHSA. Especially in FA2 and FA8, ~30% size reductions are found (Table 2). Such size reduction can disrupt or impede FA binding to these sites. FA2 and FA8, located between subdomains IA and IIA and between subdomain IB and IIIA, respectively, (Figure 1) are dwindled due to the twisting motion that causes the inward movement of domains I and III. This finding highlights the loss of FA binding capability and also explains why glycated albumin was found to lose its FA binding ability in the previous experimental studies.⁵⁵

Table 2 Solvent accessible surface areas of nine fatty acid sites (FA1-FA9) with standard deviation.

FA-binding site	HSA (PDB:1AO6)	SCH1	SCH2	AMA1	AMA2
FA1	12.951	10.86±0.34	10.03±0.52	10.82±0.35	10.71±0.38
FA2	11.246	7.56±0.52	7.32±0.26	8.54±0.41	7.85±0.51
FA3,FA4	17.214	13.20±0.26	13.13±0.26	13.04±0.26	13.10±0.34
FA5	8.712	6.10±0.25	6.53±0.47	6.51±0.42	6.18±0.33
FA6	7.096	5.79±0.19	5.83±0.15	5.79±0.17	5.73±0.20
FA7	7.841	6.41±0.16	6.46±0.16	6.40±0.16	6.38±0.15
FA8	16.235	12.70±0.52	13.47±0.41	13.25±0.40	13.14±0.40
FA9	7.349	5.71±0.36	5.57±0.33	5.94±0.33	5.60±0.33

GHSA binding site characteristics

Finally, the binding mechanisms of both sugars are investigated. As mentioned earlier, the release of GLC in SCH is observed, while GLC in AMA remains inside Sudlow's site I throughout the course of simulations (Figure 5). It can be seen that GLO is more mobile in

SCH than AMA (Figure 5A). The high mobility of GLO chain in SCH causes less interactions with the protein and eventually more water exposure, compared to the case in AMA (Table 3). In the case of GLC, both SCH and AMA show similar numbers of protein and water contacts (Table 3). Thus, the hydrogen bonds with protein and water cannot be used to distinguish the stability of GLC inside a pocket of both glycosylated forms. However, one of the key factors that can differentiate SCH from AMA is the formation of sugar-sugar dimer which is only seen in SCH (Figure 6). The high flexibility and more water exposure of GLO seen in SCH can facilitate the GLO-GLC pairing and initiate the delocalization of GLC which leads to the dissociation of GLC in SCH (Figure 5A). Note that GLC in AMA has similar number of albumin and water interactions as GLC in SCH (Table 3). The more rigid GLO chain in AMA and no sugar-sugar contact allow GLC to be localized inside a pocket (Table 3 and Figure 5A and 6). Consequently, the GLO flexibility and sugar-sugar dimer formation seems to define the binding capability of GLC to Sudlow's site I.

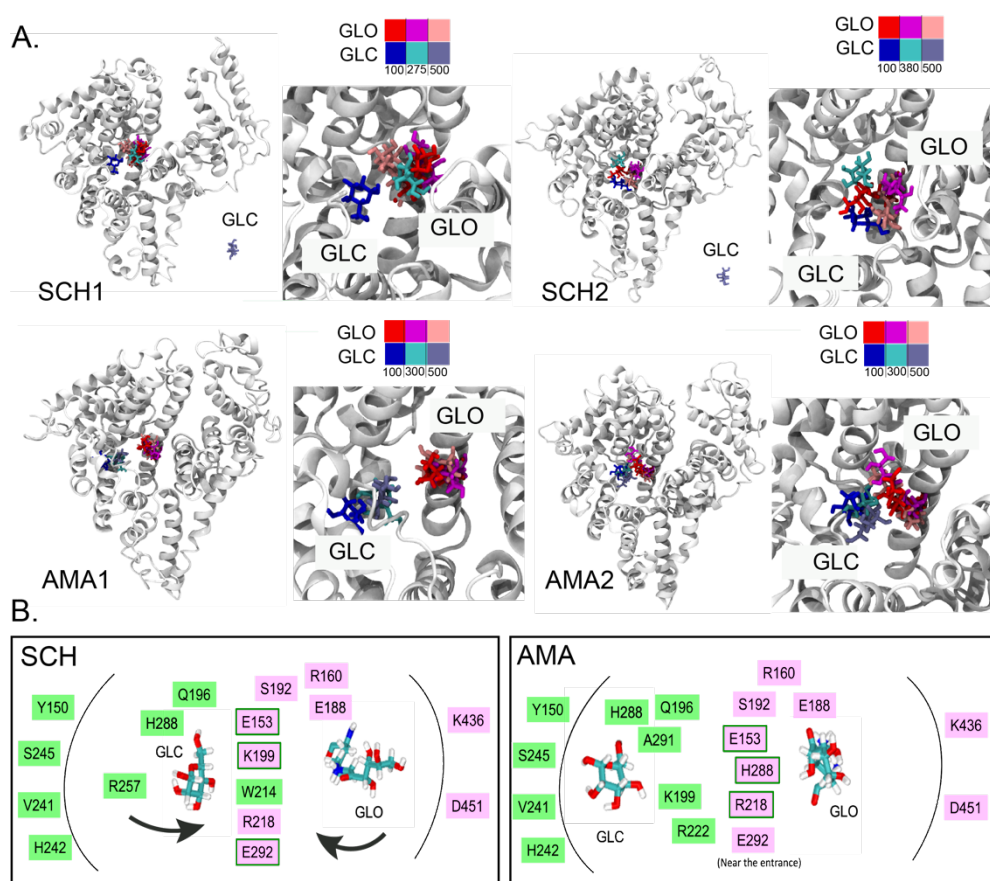


Figure 5 (A) Cartoon views of GLO and GLC displacements as a function of time for all systems. (B) Architectures of Sudlow's site I where residues interacting with GLO and GLC are labelled in pink and green, respectively. Pink boxes with green edge refer to residues that

can interact with both GLO and GLC. Two curved lines stand for the wall of binding cavity. The arrows indicate the direction of GLO and GLC movement in SCH.

Table 3 Number of hydrogen bonds for sugar-sugar, sugar-protein, and sugar-water in all systems.

	SCH1	SCH2	AMA1	AMA2
GLO-Protein	1.98±1.17	1.58±1.53	2.40±0.97	2.89±1.17
GLO-water	5.28±1.67	5.15± 1.66	4.83±1.52	4.18±1.85
GLC-Protein	3.98±1.30	3.09 ±1.41	2.40±1.21	3.23±1.02
GLC-water	4.28±1.61	5.06 ±1.84	5.12±1.49	4.97±1.67

The nature of GLC and GLO inside the drug-binding site is further investigated. In both GHSA forms, the GLC displacement inside a pocket is found due to the large cavity of Sudlow's site I. This GLC displacement was also found in our previous non-covalently bound glucose-albumin studies^{40,54}. The orientations of each sugar as a function of time can be seen in Figure S5 and S6 in supplementary information. GLCs in both SCH and AMA seem to bind at different locations. GLC in AMA is more buried inside a pocket, whereas GLC in SCH moves toward the pocket entrance (Figure 5B). The sugar-residue interactions can be seen in Figure 6. In SCH, the flexible GLO chain permits it to relocate from the right to the center of a pocket (Figure 5B). GLO in SCH1 breaks down the interactions with S192, K436, and D451 displace to the center of a pocket by forming a new interaction network with E153, R160, E292 (Figure 6). The long-lasting interaction with E188 in SCH1 indicates its role in sweeping GLO from the right to the center of a pocket (Figure 5B,6). For GLO in SCH2, it stays in a similar zone to that in SCH1, but GLO seems to diffuse inside the pocket by transient hydrogen bonds to R160, E188, R218, E292, and D451 (Figure 5B and 6). In the case of GLC, both GLCs in SCHs exit the pocket at ~300 ns (SCH1) and ~400 ns (SCH2). These GLCs are initially located at the center of the pocket and interact with E153, S192, K195, Q196, K199, W214, R128, H242, R257, H288, E292, D451 (Figure 6). GLC can also form a hydrogen bond with the GLO-K195 complex. It is clear in Figure 6 that the GLO-GLC dimer formation disrupts the GLC-protein interactions at the left of the pocket wall, leading to the relocation of GLC to the middle region (Figure 5B,6). Evidently, the long and flexible GLO-K195 chain in SCH does not only

drag GLC out to the center, but, in assistance with K199 and E292, it also sweeps GLC to the pocket entrance and results in the GLC release.

Unlike SCH, GLC in AMA moves towards the left wall and gets stabilized by Y150, E153, Q196, K199, R218, R222, H242, R257, S287, H288, A291, and E292 (Figure 6). The displacement of GLC inside a pocket is also seen in GLC in SCH, but GLC in AMA seems to be permanently tethered by Q196, K199, and H242 in AMA1 and E153, K199, and E292 in AMA2 (Figure 5B,6). This interaction network can strongly trap GLC inside Sudlow's site I. Furthermore, the absence of GLO-GLC dimer formation in AMA appears to sustain the GLC-protein complex. For GLO in AMA, its sidechain appears to point towards the pocket entrance and forms hydrogen bonds with E153, E188, S192, R218, H288, and E292 (Figure 5B,6). Especially, E188 and E292 are the main contributor for anchoring GLO at the center, resulting in the enhancement of GLO rigidity in AMA, whereas the interactions with E188 and E292 are transient in SCH and leads to the flexible GLO chain (Figure 6).

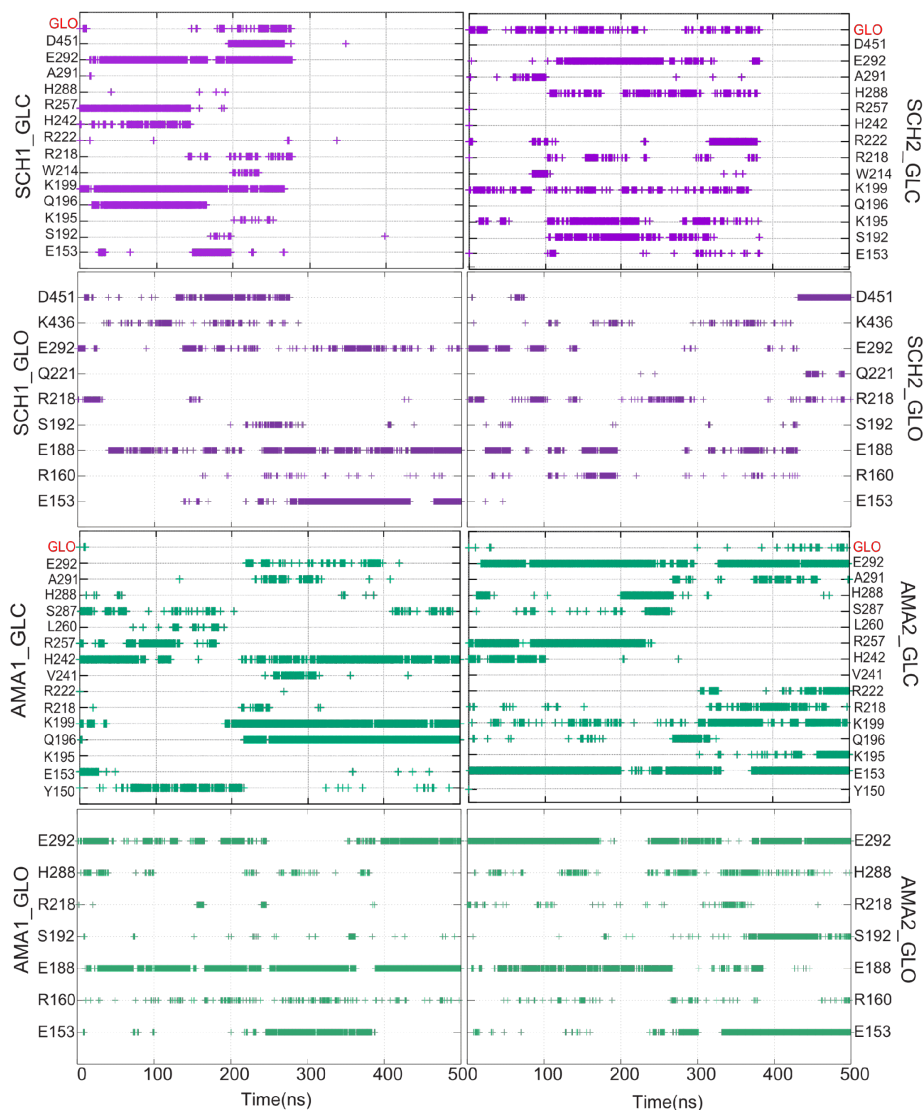


Figure 6 Number of hydrogen bonds as a function of time between sugar molecules (GLO and GLC) and key residues.

To investigate the route of GLC exit in SCH, the dimension of the pocket entrance is measured (Figure 7). As reported above, the glycation causes the twisting movement of domains I and III. This twisting motion shifts domain I inwardly, resulting in the dimensional change of the mouth of Sudlow's site I (Figure 7A). The decrease of F156-E294 and E188-C448 C_{α} - C_{α} distances (Figure 7BC) demonstrates the inward movement of domain I in all cases. The distance between E294 and C448 at the entrance is used to determine the width of the pocket entrance (Figure 7D). The longer E294-C448 distance in SCH suggests the widening of Sudlow's site's mouth in SCH, while the domain movement causes the insignificant change in E294-C448 distance of AMA. Apparently, the high mobility of GLO chain and enlargement of the pocket entrance in SCH facilitate the exit of GLC. In contrast, the preserved mouth dimension and more rigid GLO allow GLC in AMA to be kept stably inside the pocket.

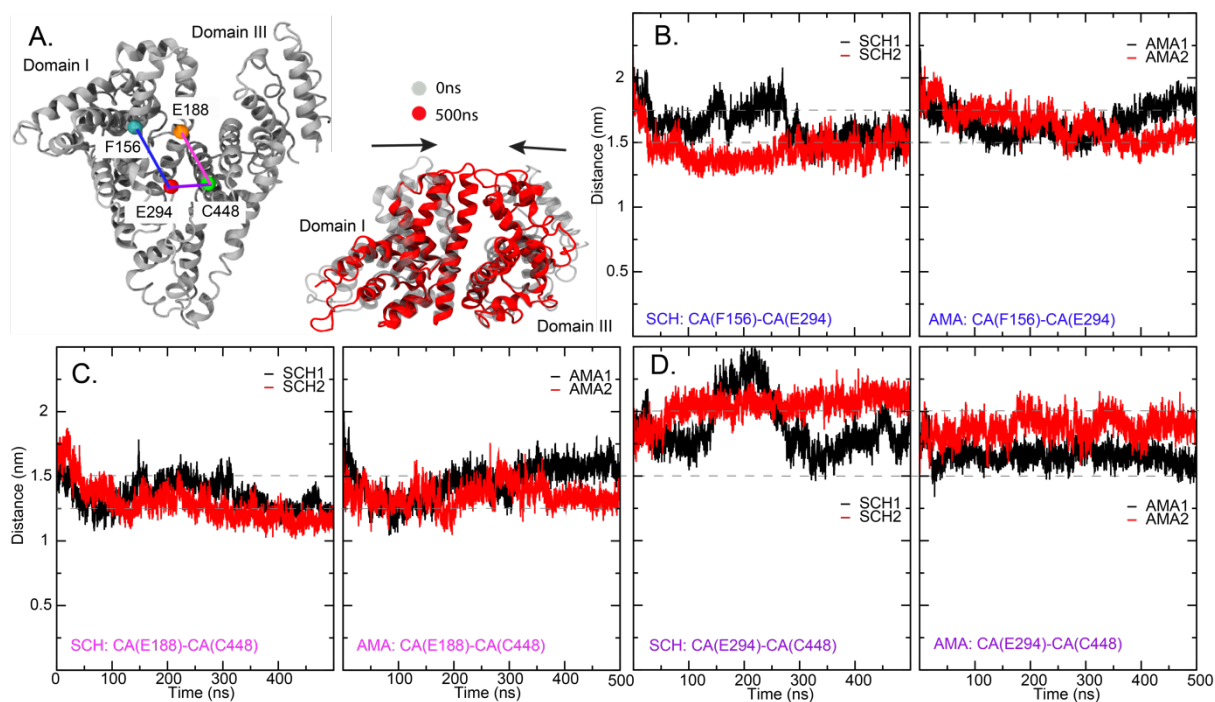


Figure 7 (A) Location of C_{α} of residues used to measure the entrance dimension (E188, F156, E294, and C448) of Sudlow's site I (left) and the bottom view of the inward movement of domains I and III (right). C_{α} - C_{α} distances of F156-E294 (B), E188-C448 (C), and E294-C448 (D).

Conclusion

The current work confirms that the glycation causes the alteration in HSA structure and function which have been reported in previous experimental works ^{2, 56}. Many studies have

reported the loss of drug binding affinity and structural changes during the glycation^{26,57-59}, but no molecular detail was provided. Herein, we found that the glycation at Sudlow's site I does not only cause the helical unfolding, especially at domains I and III, but also alter the protein dynamics. The twisting motion of GHSA causes domains I and III to move in an inward direction. This motion also induces a number of changes, i.e., (i) the widening of Sudlow's site I entrance, (ii) the size reduction of nine FA-binding pockets, (iii) the enlargement of Sudlow's site I and the reduction of Sudlow's site II, (iv) the enhancement of C34 reactivity, and (v) the change in W214 microenvironment. SCH seems to disrupt the structure and function of GHSA more than AMA. Glycated albumin has been recognized as a potential biomarker for diabetes mellitus^{2, 60-62}, chronic kidney diseases⁶³⁻⁶⁵, and antineutrophil cytoplasmic antibody-associated vasculitis (AAV).⁶⁶ Many attempts have been made to detect GHSA quantity⁶⁷⁻⁷¹. One of the key bottlenecks for the effective GHSA-detecting strategy is to differentiate GHSA from native HSA in a sample. Therefore, the structural and dynamic insights obtained here will benefit the design of specific and selective strategies for GHSA detection. Nevertheless, here the effect of glycation was studied for only one site, K195. The microscopic impact of multiple glycation on albumin structure and function thus remains to be investigated.

Supporting Information

Supplementary is available free of charge at

The RESP charges distribution of GLO-K195 complex in the Schiff base and the Amadori product (Figure S1), cartoon representation of PCA analysis of SCH and AMA (Figure S2), radius of gyration (Rg) (Figure S3), Dihedral angles of W214 in the pocket (Figure S4), structural map of the sugar rearrangement inside the pocket as a function of simulation time in SCH (Figure S5) and AMA (Figure S6)

Acknowledgement

This research was financially supported by Kasetsart University Research and Development Institute (KURDI, grant no. FF(KU) 25.64), National Science and Technology Development Agency (NSTDA) (Grant No. P2251069), National Research Council of Thailand (NRCT), The Agricultural Research Development Agency (Public Organization), and Grant-in-Aid for Scientific Research (22H02035). SS would like to acknowledge the Royal Golden Jubilee (RGJ) Ph. D. Programme (PHD/0131/2561) and the Capacity Building of KU Students on Internationalization Program (KUCSI) for financial support. The calculations were partially

carried out at the Research Center for Computational Sciences in Okazaki (Project: 22-IMS-C123), Research Institute for Information Technology, Kyushu University (category of General Projects), and NSTDA supercomputer center (ThaiSC).

References

- (1) Kaul, K.; Tarr, J. M.; Ahmad, S. I.; Kohner, E. M.; Chibber, R., Introduction to Diabetes Mellitus. *Adv. Exp. Med. Biol.* **2012**, 771, 1-11.
- (2) Anguizola, J.; Matsuda, R.; Barnaby, O. S.; Hoy, K. S.; Wa, C.; DeBolt, E.; Koke, M.; Hage, D. S., Review: Glycation of Human Serum Albumin. *Clin Chim Acta* **2013**, 425, 64-76.
- (3) Mohamed, W. R.; Mahmoud, N.; Abdel Samad, F.; Ahmed, E.; Hamblin, M. R.; Mohamed, T., Rapid Monitoring of Serum Albumin as a Biomarker of Liver and Kidney Diseases Using Femtosecond Laser-Induced Fluorescence. *Spectrochimica Acta Part A*: **2022**, 268, 120646.
- (4) Hemmati Dinarvand, M.; Saedi, S.; Kalantary-Charvadeh, A.; Bagheri, s.; Mota, A.; Valiloo, M., Evaluation of the Serum Concentrations of Albumin and Uric Acid as a Biomarker in Patients With Parkinson's Disease. *Yafteh* **2018**, 20, 39-47.
- (5) Bai, Y.; Fang, Y.; Ming, J.; Wei, H.; Zhang, P.; Yan, J.; Du, Y.; Li, Q.; Yu, X.; Guo, M.; et al. Serum Glycated Albumin as Good Biomarker for Predicting Type 2 Diabetes: A Retrospective Cohort Study of China National Diabetes and Metabolic Disorders Survey. *Adv. Exp. Med. Biol.* **2022**, 38, e3477.
- (6) Raghav, A.; Ahmad, J., Glycated Serum Albumin: A Potential Disease Marker and an Intermediate Index of Diabetes Control. *Diabetes Metab. Syndr: Clin. Res. Rev.* **2014**, 8, 245-251.
- (7) Hassan, M.; Azzazy, E.; Christenson, R. H., All About Albumin: Biochemistry, Genetics and Medical Applications. *Clin. Chem.* **1997**, 43, 2014a-2015.
- (8) Czub, M. P.; Venkataramany, B. S.; Majorek, K. A.; Handing, K. B.; Porebski, P. J.; Beeram, S. R.; Suh, K.; Woolfork, A. G.; Hage, D. S.; Shabalin, I. G.; et al. Testosterone Meets Albumin - The Molecular Mechanism of Sex Hormone Transport by Serum Albumins. *Chem.* **2019**, 10, 1607-1618.
- (9) Shamsi, A.; Ahmed, A.; Khan, M. S.; Al Shahwan, M.; Husain, F. M.; Bano, B., Understanding the Binding Between Rosmarinic Acid and Serum Albumin: In Vitro and In Silico Insight. *J. Mol. Liq.* **2020**, 311, 113348.
- (10) Yang, F.; Zhang, Y.; Liang, H., Interactive Association of Drugs Binding to Human Serum Albumin. *Int J Mol Sci* **2014**, 15, 3580-3595.
- (11) Rahnema, E.; Mahmoodian-Moghaddam, M.; Khorsand-Ahmadi, S.; Saberi, M. R.; Chamani, J., Binding Site Identification of Metformin to Human Serum Albumin and Glycated Human Serum Albumin by Spectroscopic and Molecular Modeling Techniques: A Comparison Study. *J. Biomol. Struct. Dyn.* **2015**, 33, 513-533.
- (12) Li, Q.; Yang, W.; Qu, L.; Qi, H.; Huang, Y.; Zhang, Z., Interaction of Warfarin With Human Serum Albumin and Effect of Ferulic Acid on the Binding. *J Spectrosc* **2014**, 2014, 834501.
- (13) Ghuman, J.; Zunszain, P. A.; Petitpas, I.; Bhattacharya, A. A.; Otagiri, M.; Curry, S., Structural Basis of the Drug-binding Specificity of Human Serum Albumin. *J. Mol. Biol.* **2005**, 353, 38-52.
- (14) Sudlow, G.; Birkett, D. J.; Wade, D. N., The Characterization of Two Specific Drug Binding Sites on Human Serum Albumin. *Mol. Pharmacol.* **1975**, 11, 824-832.
- (15) Sudlow, G.; Birkett, D. J.; Wade, D. N., Further Characterization of Specific Drug Binding Sites on Human Serum Albumin. *Mol. Pharmacol.* **1976**, 12, 1052-1061.
- (16) Bhattacharya, A. A.; Grüne, T.; Curry, S., Crystallographic Analysis Reveals Common Modes of Binding of Medium and Long-Chain Fatty Acids to Human Serum Albumin. *J Mol Biol* **2000**, 303, 721-732.
- (17) Xing, H.; Yaylayan, V., Mechanochemical Generation of Schiff Bases and Amadori Products and Utilization of Diagnostic Ms/Ms Fragmentation Patterns in Negative Ionization Mode for Their Analysis. *Carbohydr. Res.* **2020**, 495, 108091.
- (18) Xing, H.; Mossine, V. V.; Yaylayan, V., Diagnostic Ms/Ms Fragmentation Patterns for the Discrimination Between Schiff Bases and Their Amadori or Heyns Rearrangement Products. *Carbohydr. Res.* **2020**, 491, 107985.

- (19) Cao, H.; Chen, T.; Shi, Y., Glycation of Human Serum Albumin in Diabetes: Impacts on the Structure and Function. *Curr. Med. Chem.* **2015**, *22*, 4-13.
- (20) Nasiri, R.; Bahrami, H.; Zahedi, M.; Moosavi-Movahedi, A. A.; Sattarahmady, N., A Theoretical Elucidation of Glucose Interaction With HSA's Domains. *J. Biomol. Struct. Dyn.* **2010**, *28*, 211-226.
- (21) Neelofar, K.; Ahmad, J., An Overview of in Vitro and in Vivo Glycation of Albumin: A Potential Disease Marker in Diabetes Mellitus. *Glycoconj. J.* **2017**, *34*, 575-584.
- (22) Wang, Y.; Yu, H.; Shi, X.; Luo, Z.; Lin, D.; Huang, M., Structural Mechanism of Ring-Opening Reaction of Glucose by Human Serum Albumin. *J Biol Chem.* **2013**, *288*, 15980-15987.
- (23) Ahmed, N. Advanced Glycation Endproducts—Role in Pathology of Diabetic Complications. *Diabetes Res Clin Pract* **2005**, *67*, 3-21.
- (24) Baraka-Vidot, J.; Guerin-Dubourg, A.; Bourdon, E.; Rondeau, P., Impaired Drug-Binding Capacities of in Vitro and in Vivo Glycated Albumin. *Biochimie* **2012**, *94*, 1960-1967.
- (25) Arif, B.; Ahmad, Z.; Bhat, G.; Mudassar, S.; Aalam, K., Biophysical Characterisation of Amadori Modified Human Serum Albumin: A Prognostic Biomarker for Diabetic Complications. *J Clin of Diagn Res* **2022**, *16*, BC01-BC06.
- (26) Ahmed, A.; Shamsi, A.; Khan, M. S.; Husain, F. M.; Bano, B., Methylglyoxal induced glycation and aggregation of human serum albumin: Biochemical and biophysical approach. *Int. J. Biol. Macromol* **2018**, *113*, 269-276.
- (27) Al Jaseem, M. A. J.; Abdullah, K. M.; Qais, F. A.; Shamsi, A.; Naseem, I., Mechanistic Insight into Glycation Inhibition of Human Serum Albumin by Vitamin B9: Multispectroscopic and Molecular Docking Approach. *Int. J. Biol. Macromol.* **2021**, *181*, 426-434.
- (28) Dennington, R.; Keith, T.; Millam, J. *GaussView*, Version 6.1, Semichem Inc., Shawnee Mission, KS, 2016.
- (29) Frisch, M. J.; Trucks, G. W.; Schlegel, H. B.; Scuseria, G. E.; Robb, M. A.; Cheeseman, J. R.; Scalmani, G.; Barone, V.; Petersson, G. A.; Nakatsuji, H. et al. *Gaussian 16 Rev. C.01*, Wallingford, CT, 2016
- (30) Case D.A., Aktulga H. M., Belfon K., Ben-Shalom I.Y., Brozell S.R., Cerutti D.S., Cheatham T.E. III, Cruzeiro V.W.D., Darden T.A., Duke R.E. et la. *AmberTools2020*; University of California, SF, 2020
- (31) Lindorff-Larsen, K.; Piana, S.; Palmo, K.; Maragakis, P.; Klepeis, J. L.; Dror, R. O.; Shaw, D. E., Improved Side-Chain Torsion Potentials for the Amber FF99SB Protein Force Field. *Proteins* **2010**, *78*, 1950-1958.
- (32) Wang, J. Wolf, R. M.; Caldwell, J. W.; Kollman, P. A.; Case, D. A., Development and Testing of a General Amber Force Field. **2004**, *25*, 1157-1174.
- (33) Sousa da Silva, A. W.; Vranken, W. F., ACPYPE - AnteChamber PYthon Parser interfacE. *BMC Research Notes* **2012**, *5*, 367.
- (34) Van Der Spoel, D.; Lindahl, E.; Hess, B.; Groenhof, G.; Mark, A. E.; Berendsen, H. J. C., GROMACS: Fast, Flexible, and Free. *J. Comput. Chem.* **2005**, *26*, 1710-1718.
- (35) Darden, T.; York, D.; Pedersen, L., Particle Mesh Ewald: An N·Log(N) Method for Ewald Sums in Large Systems. *Chem. Phys.* **1993**, *98*, 10089-10092.
- (36) Humphrey, W.; Dalke, A.; Schulten, K., VMD: Visual Molecular Dynamics. *J. Mol. Graph.* **1996**, *14*, 33-38.
- (37) Xiao, S.; Tian, H.; Tao, P., PASSer2.0: Accurate Prediction of Protein Allosteric Sites Through Automated Machine Learning. *Front. Mol. Biosci.* **2022**, *9*.
- (38) Pongprayoon, P.; Gleeson, M. P., Probing the Binding Site Characteristics of HSA: A Combined Molecular Dynamics and Cheminformatics Investigation. *J. Mol. Graph. Model.* **2014**, *54*, 164-173.
- (39) Awang, T.; Niramitranon, J.; Japrun, D.; Saparpakorn, P.; Pongprayoon, P., Investigating the Binding Affinities of Fructose and Galactose to Human Serum Albumin: Simulation Studies. *Mol Simul.* **2021**, *47*, 738 - 747.
- (40) Pongprayoon, P.; Mori, T., The Critical Role of Dimer Formation in Monosaccharides Binding to Human Serum Albumin. *Phys. Chem. Chem. Phys.* **2018**, *20*, 3249-3257.

- (41) Ketrat, S.; Japrun, D.; Pongprayoon, P., Exploring How Structural and Dynamic Properties of Bovine and Canine Serum Albumins Differ From Human Serum Albumin. *J. Mol. Graph. Model.* **2020**, *98*, 107601.
- (42) Somboon, K.; Niramitranon, J.; Pongprayoon, P., Probing the Binding Affinities of Imipenem and Ertapenem for Outer Membrane Carboxylate Channel D1 (Ocd1) From *P. Aeruginosa*: Simulation Studies. *J. Mol. Model.* **2017**, *23*, 227.
- (43) Pongprayoon, P.; Japrun, D., Revealing the Structural Dynamics of Feline Serum Albumin. *Struct. Chem.* **2021**, *32*, 69-77.
- (44) Bohlooli, M.; Ghaffari-Moghaddam, M.; Khajeh, M.; Sheibani, N., Determination of Amadori Product in Glycated Human Serum Albumin by Spectroscopy Methods. *ChemistrySelect* **2018**, *3*, 7018-7022.
- (45) Bohlooli, M.; Moosavi-Movahedi, A. A.; Taghavi, F.; Saboury, A. A.; Maghami, P.; Seyedarabi, A.; Moosavi-Movahedi, F.; Ahmad, F.; Shockravi, A.; Habibi-Rezaei, M., Inhibition of Fluorescent Advanced Glycation End Products (AGEs) of Human Serum Albumin Upon Incubation With 3-B-Hydroxybutyrate. *Mol Biol Rep* **2014**, *41*, 3705-3713.
- (46) Bujacz, A., Structures of Bovine, Equine and Leporine Serum Albumin. *Acta Crystallogr. D Biol.* **2012**, *68*, 1278-1289.
- (47) Anraku, M.; Chuang, V. T.; Maruyama, T.; Otagiri, M., Redox Properties of Serum Albumin. *Biochim Biophys Acta* **2013**, *1830*, 5465-5472.
- (48) Shojai, S.; Haeri Rohani, S. A.; Moosavi-Movahedi, A. A.; Habibi-Rezaei, M., Human Serum Albumin in Neurodegeneration. *Annu. Rev. Neurosci.* **2022**, *33*, 803-817.
- (49) Bonanata, J.; Turell, L.; Antmann, L.; Ferrer-Sueta, G.; Botasini, S.; Méndez, E.; Alvarez, B.; Coitiño, E. L., The Thiol of Human Serum Albumin: Acidity, Microenvironment and Mechanistic Insights on Its Oxidation to Sulfenic Acid. *Free Radic. Biol. Med.* **2017**, *108*, 952-962.
- (50) Niramitranon, J.; Japrun, D.; Boonmee, A.; Koonawootrittriron, S.; Suwanasopee, T.; Jattawa, D.; Pongprayoon, P., Dynamic and Structural Properties of Porcine Serum Albumins. *Mol. Simul* **2023**, 1-8
- (51) Szkudlarek, A.; Wilk, M.; Maciążek-Jurczyk, M., In Vitro Investigations of Acetohexamide Binding to Glycated Serum Albumin in the Presence of Fatty Acid. *Molecules* **2020**, *25*.
- (52) Szkudlarek, A.; Pożycka, J.; Kulig, K.; Owczarzy, A.; Rogóż, W.; Maciążek-Jurczyk, M. Changes in Glycated Human Serum Albumin Binding Affinity for Losartan in the Presence of Fatty Acids In Vitro Spectroscopic Analysis. *Molecules*. **2022**, *27*. 401
- (53) Szkudlarek, A.; Pożycka, J.; Maciążek-Jurczyk, M., Influence of Piracetam on Gliclazide-Glycated Human Serum Albumin Interaction. A Spectrofluorometric Study. *Molecules* **2018**, *24*.
- (54) Awang, T.; Wiriyatanakorn, N.; Saparpakorn, P.; Japrun, D.; Prapasiri, P., Understanding the Effects of Two Bound Glucose in Sudlow Site I on Structure and Function of Human Serum Albumin: Theoretical Studies. *J. Biomol.* **2017**, *35*, 781-790.
- (55) Blache, D.; Bourdon, E.; Salloignon, P.; Lucchi, G.; Ducoroy, P.; Petit, J. M.; Verges, B.; Lagrost, L., Glycated Albumin With Loss of Fatty Acid Binding Capacity Contributes to Enhanced Arachidonate Oxygenation and Platelet Hyperactivity: Relevance in Patients With Type 2 Diabetes. *Diabetes* **2015**, *64* (3), 960-72.
- (56) Iberg, N.; Flückiger, R., Nonenzymatic Glycosylation of Albumin in Vivo. Identification of Multiple Glycosylated Sites. *J Biol Chem* **1986**, *261*, 13542-14545.
- (57) Joseph, K. S.; Anguizola, J.; Jackson, A. J.; Hage, D. S., Chromatographic Analysis of Acetohexamide Binding to Glycated Human Serum Albumin. *J Chromatogr B Analyt Technol Biomed Life Sci* **2010**, *878*, 2775-2781.
- (58) Anguizola, J. A.; Basiaga, S. B.; Hage, D. S., Effects of Fatty Acids and Glycation on Drug Interactions With Human Serum Albumin. *Curr Metabolomics* **2013**, *1*, 239-250.
- (59) Joseph, K. S.; Anguizola, J.; Hage, D. S., Binding of Tolbutamide to Glycated Human Serum Albumin. *J Pharm Biomed Anal* **2011**, *54*, 426-32.
- (60) Inaba, M.; Okuno, S.; Kumeda, Y.; Yamada, S.; Imanishi, Y.; Tabata, T.; Okamura, M.; Okada, S.; Yamakawa, T.; Ishimura, E.; et al. Glycated Albumin is a Better Glycemic Indicator Than Glycated Hemoglobin Values in Hemodialysis Patients With Diabetes: Effect of Anemia and Erythropoietin Injection. *J. Am. Soc. Nephrol.* **2007**, *18*, 896-903.

- (61) Yoshiuchi, K.; Matsuhisa, M.; Katakami, N.; Nakatani, Y.; Sakamoto, K.; Matsuoka, T.; Umayahara, Y.; Kosugi, K.; Kaneto, H.; Yamasaki, Y., et al. Glycated Albumin is a Better Indicator for Glucose Excursion Than Glycated Hemoglobin in Type 1 and Type 2 Diabetes. *Endocr. J.* **2008**, *55*, 503-507.
- (62) Guerin-Dubourg, A.; Catan, A.; Bourdon, E.; Rondeau, P., Structural Modifications of Human Albumin in Diabetes. *Diabetes Metab J* **2012**, *38*, 171-178.
- (63) Lim, P. S.; Cheng, Y. M.; Yang, S. M., Impairments of The Biological Properties of Serum Albumin in Patients on Haemodialysis. *Nephrology (Carlton, Vic.)* **2007**, *12*, 18-24.
- (64) Kawai, Y.; Masutani, K.; Torisu, K.; Katafuchi, R.; Tanaka, S.; Tsuchimoto, A.; Mitsuki, K.; Tsuruya, K.; Kitazono, T., Association Between Serum Albumin Level and Incidence of End-Stage Renal Disease in Patients With Immunoglobulin a Nephropathy: A Possible Role of Albumin as an Antioxidant Agent. *PLoS One* **2018**, *13*, e0196655.
- (65) Lang, J.; Katz, R.; Ix, J. H.; Gutierrez, O. M.; Peralta, C. A.; Parikh, C. R.; Satterfield, S.; Petrovic, S.; Devarajan, P.; Bennett, M.; et al. Association of Serum Albumin Levels With Kidney Function Decline and Incident Chronic Kidney Disease in Elders. *Nephrol. Dial. Transplant.* **2018**, *33*, 986-992.
- (66) Park, P. G.; Pyo, J. Y.; Ahn, S. S.; Song, J. J.; Park, Y. B.; Lee, S. W., Serum Glycated Albumin as a Predictive Biomarker for Renal Involvement of Antineutrophil Cytoplasmic Antibody-Associated Vasculitis in Non-Diabetic Patients. *BMC Nephrol.* **2022**, *23*, 288.
- (67) Apiwat, C.; Luksirikul, P.; Kankla, P.; Pongprayoon, P.; Treerattrakoon, K.; Paiboonsukwong, K.; Fucharoen, S.; Dharakul, T.; Japrun, D., Graphene Based Aptasensor for Glycated Albumin in Diabetes Mellitus Diagnosis and Monitoring. *Biosens.* **2016**, *82*, 140-145.
- (68) Aye, N. N.; Maraming, P.; Tavichakorntrakool, R.; Chaibunruang, A.; Boonsiri, P.; Daduang, S.; Teawtrakul, N.; Prasongdee, P.; Amornkitbamrung, V.; Daduang, J. A Simple Graphene Functionalized Electrochemical Aptasensor for the Sensitive and Selective Detection of Glycated Albumin. *Appl. Sci.*, **2021**, *11*, 10315
- (69) Bunyarataphan, S.; Dharakul, T.; Fucharoen, S.; Paiboonsukwong, K.; Japrun, D., Glycated Albumin Measurement Using an Electrochemical Aptasensor for Screening and Monitoring of Diabetes Mellitus. *Electroanalysis* **2019**, *31*, 2254-2261.
- (70) Sasar, M.; Farzadfard, A.; Abdi, Y.; Habibi-Rezaei, M., Detection of Glycated Albumin Using a Novel Field Effect Aptasensor. *IEEE Sens. J.* **2020**, *20*, 10387-10392.
- (71) Ki, H., Oh, J., Hana, G., Kim M., Glycation Ratio Determination Through Simultaneous Detection of Human Serum Albumin and Glycated Albumin on an Advanced Lateral Flow Immunoassay Sensor. *Lab Chip* **2020**, *20*, 844-851.

TOC graphic

